ARTICLES

Spatial organization of the flow of genetic information in bacteria

Paula Montero Llopis[1]*, Audrey F. Jackson[1]*†, Oleksii Sliusarenko[1,2], Ivan Surovtsev[2], Jennifer Heinritz[2], Thierry Emonet[1,3] & Christine Jacobs-Wagner[1,2,4]

Eukaryotic cells spatially organize mRNA processes such as translation and mRNA decay. Much less is clear in bacterial cells where the spatial distribution of mature mRNA remains ambiguous. Using a sensitive method based on quantitative fluorescence *in situ* hybridization, we show here that in *Caulobacter crescentus* and *Escherichia coli*, chromosomally expressed mRNAs largely display limited dispersion from their site of transcription during their lifetime. We estimate apparent diffusion coefficients at least two orders of magnitude lower than expected for freely diffusing mRNA, and provide evidence in *C. crescentus* that this mRNA localization restricts ribosomal mobility. Furthermore, *C. crescentus* RNase E appears associated with the DNA independently of its mRNA substrates. Collectively, our findings show that bacteria can spatially organize translation and, potentially, mRNA decay by using the chromosome layout as a template. This chromosome-centric organization has important implications for cellular physiology and for our understanding of gene expression in bacteria.

In bacterial cells, the major mRNA species is the full-length transcript. Its predominance over nascent, partially transcribed mRNA is supported by northern blotting and recently by quantitative deep RNA sequencing of an entire bacterial transcriptome showing that 3′ and 5′ regions of transcripts have similar representation[1]. Transcription rate measurements (approximately 25–80 nucleotides per second[2,3]) are consistent with this view; for example, a 1-kilobase gene is transcribed in about 20 s, which is shorter than the known half-lives of most mRNAs (between 3 and 8 min for ~80% of *E. coli* transcripts[4]). These results indicate that, although ribosome binding and translation are initiated on the nascent mRNA in bacteria[5], the bulk of translation occurs on mature transcripts, which are generally assumed to diffuse freely inside cells. Studies using plasmids have estimated apparent diffusion coefficients (D_a) of mRNA to be between 0.03 and 0.3 $\mu m^2 s^{-1}$ in bacteria[6,7], these values are sufficient to disperse mRNAs throughout the cell before degradation. This would imply that synthesis of any particular protein occurs at random cellular locations, as current models of gene expression assume.

Bacterial mRNAs are present in very low copy numbers[1], making their visualization inside cells challenging. Creative methods have been developed to attempt to detect specific mRNAs or to quantify their levels and temporal fluctuations in cells[6–12]. Although they provide interesting biological information, these studies were not designed to probe the localization of chromosomally encoded mRNA and/or lacked spatial resolution and positional references such as transcription sites. They also led to a very confusing picture of mRNA localization, possibly because the mRNA was often expressed from heterologous promoters and plasmids[6,7,9,10,12], and because some methods caused long-lived fluorescent signals[7,9,10,12], inconsistent with the short half-lives of bacterial mRNAs[4]. Consequently, the localization of mRNA in bacterial cells remains poorly characterized.

mRNA localization in *C. crescentus* and *E. coli*

Our goal was to visualize and quantify the spatial distribution of specific chromosomally expressed mRNAs under conditions in which mRNA is synthesized and degraded normally. We first aimed to visualize, in *C. crescentus*, the naturally abundant *groESL* mRNA, which encodes two chaperones essential for viability under normal growth conditions[13]. For detection of *groESL* transcripts, we used fluorescence *in situ* hybridization (FISH) microscopy with a single locked nucleic acid (LNA)-containing probe complementary to the *groESL* mRNA sequence. Surprisingly, the fluorescent signal largely accumulated in one or two distinct foci in most cells (Fig. 1a), despite the known relative abundance of *groESL* mRNA. We observed similar localization patterns of mRNA in live *C. crescentus* cells using the MS2–GFP (bacteriophage MS2 coat protein fused to green fluorescent protein) method developed in *E. coli*[7,9] that we modified by using an assembly-defective MS2 mutant[14] to avoid problems of mRNA immortalization and spurious aggregation at the poles (Supplementary Information and Supplementary Fig. 1).

These live-cell and FISH methodologies were not sensitive enough for quantitative analysis of mRNA dispersion within cells. To improve the signal-to-noise ratio, we visualized by FISH mRNAs of interest that were transcriptionally fused to a non-coding array of 120 tandem Lac operator sequences ($lacO_{120}$)[15]. Because the 5′-untranslated region (UTR) often regulates mRNA stability[16], we fused the *lacO* array at the 3′ end, shortly after the stop codon (Fig. 1b and Supplementary Information) to reduce potential effects on mRNA degradation and translation. In all cases, the $lacO_{120}$-tagged mRNA was expressed from its native promoter at the original chromosomal locus in place of the normal mRNA. RNA-FISH with a single LNA probe against the *lacO* sequence thus results in signal amplification. We validated this approach with the *groESL*–$lacO_{120}$ mRNA by first showing that the lacO probe signal (Fig. 1b) accurately reproduced the localization pattern of the natural *groESL* mRNA (Fig. 1a). The lacO fluorescent signal was RNase-sensitive and DNase-resistant (Supplementary Fig. 2a), and RNA-FISH with a probe complementary to the DNA antisense *lacO* strand sequence (lacO–Rev) gave no detectable signal (Supplementary Fig. 2b). These results indicated that

[1]Department of Molecular, Cellular and Developmental Biology, Yale University, New Haven, Connecticut 06520, USA. [2]Howard Hughes Medical Institute, Yale University, New Haven, Connecticut 06520, USA. [3]Department of Physics, Yale University, New Haven, Connecticut 06520, USA. [4]Section of Microbial Pathogenesis, Yale School of Medicine, New Haven, Connecticut 06510, USA. †Current address: Cutaneous Biology Research Center, Massachusetts General Hospital, Harvard Medical School, Charlestown, Massachusetts 02129, USA.
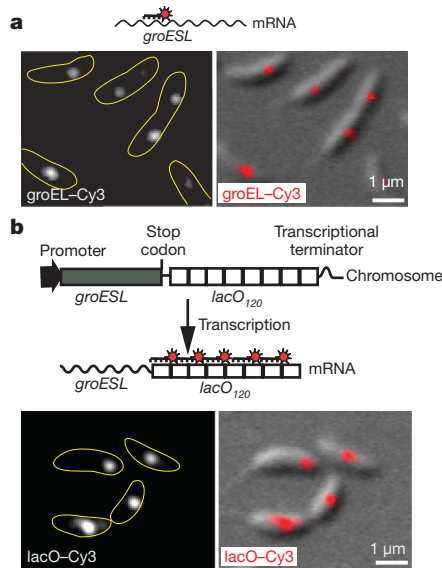*These authors contributed equally to this work.

Figure 1 | *groESL* mRNAs remain confined within subcellular regions.
a, Visualization of *groESL* mRNAs in wild-type cells by RNA FISH using a groEL–Cy3 LNA probe. **b**, Visualization of *groESL–lacO$_{120}$* mRNAs in CJW2966 cells using a lacO–Cy3 LNA probe. Note that the contrast of the lacO–Cy3 signal is scaled differently from (**a**) as it was significantly brighter.

the lacO probe hybridizes to mRNA only, and not to corresponding DNA sequences. Double labelling with the lacO probe and the internal groEL probe showed that the signals overlapped (Supplementary Fig. 2c), consistent with the two probes recognizing the same molecules. After treatment with the transcription initiation inhibitor rifampicin, the *groESL–lacO$_{120}$* mRNA signal disappeared exponentially (Supplementary Fig. 2d), with a half-time of about 3.5 ± 0.15 min (see Supplementary Information), in good agreement with real-time PCR measurements for both *groESL* and *groESL–lacO$_{120}$* mRNAs (Supplementary Information). Thus, the 3'-*lacO$_{120}$* tagging does not seem to affect *groESL* mRNA turnover.

Fluorescence intensity profiles of *groESL–lacO$_{120}$* mRNAs in individual cells (Fig. 2a) showed the quality of the mRNA signal over the background fluorescence (see Supplementary Information) and demonstrated that most *groESL–lacO$_{120}$* mRNAs are constrained within one or two subcellular regions. These regions were specific to the corresponding chromosomal sites of transcription, as shown by dual labelling of *groESL–lacO$_{120}$* mRNA and gene locus (Fig. 2b). Cells with two mRNA foci corresponded to cells after replication and segregation of the *groESL–lacO$_{120}$* gene locus. The distribution of full width at half maximum (FWHM) values of *groESL–lacO$_{120}$* mRNA peaks for the cell population (which gives a measure of the mRNA signal dispersion) was narrow, with a mean value of 0.46 ± 0.12 μm ($n = 418$; Fig. 2c). We obtained a similar FWHM distribution and mean for *groESL–lacO$_{120}$* DNA sequence using DNA FISH and the lacO–Rev probe (that can hybridize to the DNA but not the corresponding mRNA; Fig. 2c). Mean FWHM values for diffraction-limited, 175-nm green and red fluorescent microspheres were, under the same experimental conditions, 0.37 ± 0.02 μm ($n = 10$) and 0.40 ± 0.01 μm ($n = 10$), respectively. Thus, *groESL–lacO$_{120}$* mRNA displays a very restricted dispersion, close to the diffraction limit of our light microscopy setup. This indicates that the majority of *groESL* mRNAs, despite being naturally abundant relative to other transcripts, remain near their site of birth for their entire lifespan (Supplementary Fig. 2d), as opposed to being randomly mixed inside cells, as was generally assumed.

We quantified the spatial distribution of five other *C. crescentus* chromosomally encoded *lacO$_{120}$*-tagged mRNAs with varying characteristics in terms of gene location, mRNA stability and the type, location or origin of proteins produced. The *creS–lacO$_{120}$* mRNA, whose
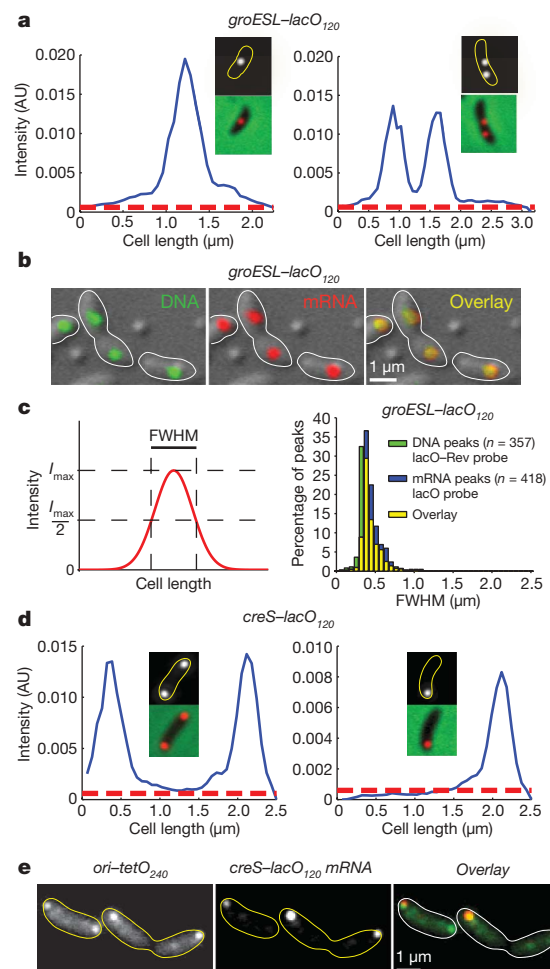

Figure 2 | *groESL* and *creS* mRNAs largely remain at the site of birth for their entire lifespan. a, Representative FISH intensity profiles of *groESL–lacO$_{120}$* mRNA (using lacO–Cy3 probe) along the cell length in individual CJW2966 cells. The red dashed line represents the background fluorescence. AU, arbitrary units. **b**, Covisualization of *groESL–lacO$_{120}$* gene locus and mRNA in CJW2969 cells. **c**, Schematic of the FWHM values obtained from intensity profiles along cell length (left); histograms of FWHM values of *groESL–lacO$_{120}$* mRNA (blue) and DNA (green) signals using RNA FISH and the lacO–Cy3 probe or DNA FISH and the lacO–Rev–FITC probe, respectively (right). **d**, Same as in (**a**) for *creS-lacO$_{120}$* mRNAs in CJW2967 cells. **e**, Co-visualization of *creS–lacO$_{120}$* mRNA and *tetO$_{240}$*-tagged DNA origins in CJW3102 cells.

gene is located near the chromosomal origin (*ori*), accumulated at the poles (Fig. 2d) and colocalized with *ori* tagged with a *tetO$_{240}$* array[17] (Fig. 2e). We obtained a similar polar accumulation of native *creS* mRNA in wild-type cells using 38 oligonucleotide probes tiled along the *creS* coding sequence (Supplementary Fig. 3; see also Supplementary Information), confirming the results obtained for the *lacO$_{120}$*-tagged mRNA using the lacO probe (Fig. 2d). *divJ–lacO$_{120}$* mRNA, which produces an inner membrane protein that is polarly localized[18], displayed little dispersion from the pole-distal locations of the *divJ* DNA locus (Supplementary Figs 4a–c and 5). Similarly, we observed limited mRNA dispersion for an outer membrane protein-encoding mRNA (*ompA–lacO$_{120}$*, Supplementary Fig. 4d–f), an exogenous mRNA producing mCherry (from a *C. crescentus Pvan* promoter at the *vanA* locus; Supplementary Fig. 4g–i), and even for the relatively long-lived flagellin *fljK* mRNA (Supplementary Fig. 4j–l), which has a reported half-life of 11 min (ref. 19). In *E. coli*, we visualized the well characterized LacZ-encoding transcripts under native conditions (that is, without any tagging) using 48 probes complementary to the *lacZ* mRNA sequence. Under steady-state isopropyl-β-D-thiogalactoside (IPTG)-inducing conditions, the monocistronic *lacZ* message, which

derives from processing of the polycistronic *lacZYA* operon mRNA, is the most abundant *lac* mRNA species as shown by northern blot[20]. In FISH experiments, the IPTG-induced *lacZ* mRNA signal formed diffraction-limited peaks (Fig. 3a, b and e) that largely colocalized with *tetO₂₅₀*-tagged DNA regions (*cynX* locus) located next to the *lac* operon (Fig. 3f). These peaks were absent in uninduced cells (Fig. 3c, d).

We do not know if our FISH methods have single-molecule sensitivity, but the signal distributions indicate that at least the majority of the transcripts remain close to their transcription site. These results were very surprising because modelling of mRNA diffusion (see Supplementary Information) predicts that most mRNA transcripts should be able to diffuse significantly from their site of transcription before being degraded. Calculations indicate that if they were freely diffusible, *groESL–lacO₁₂₀* mRNA (~6.3 kb; Fig. 4a), average-sized mRNAs of 1 kb (Supplementary Fig. 6a) or even very long mRNAs of 20 kb (Supplementary Fig. 6b) should have a largely uniform spatial profile inside the cell, whether they are free or maximally occupied by ribosomes. This is corroborated by observations that even large plasmid–protein complexes (deficient in partitioning) of comparable size to ribosome-loaded mRNAs (25–50 MDa) are highly mobile in the bacterial cytoplasm, with a D_a of about $0.02\,\mu m^2\,s^{-1}$ (ref. 21). The discrepancy between these expectations and our experimental data indicates that mRNA dispersion by diffusion is slowed by unknown physical or biochemical interactions. It has been shown that besides shape and viscosity, protein mobility can be markedly influenced by non-geometrical effects such as nonspecific electrostatic interactions[22]. Similar constraints may be at play for mRNAs.

Regardless of the precise nature of these constraints, it remained unclear whether mRNA could move at all because the mRNAs we examined produced peaks with FWHM values near or within the diffraction limit. However, when *groESL–lacO₁₂₀* cells were heat-shocked, the expected increase in *groESL–lacO₁₂₀* mRNA production[13] was accompanied with an increase in dispersion inside cells (Fig. 4b, c) that was beyond the diffraction limit (FWHM$_{mean}$ = 0.80 ± 0.19 μm
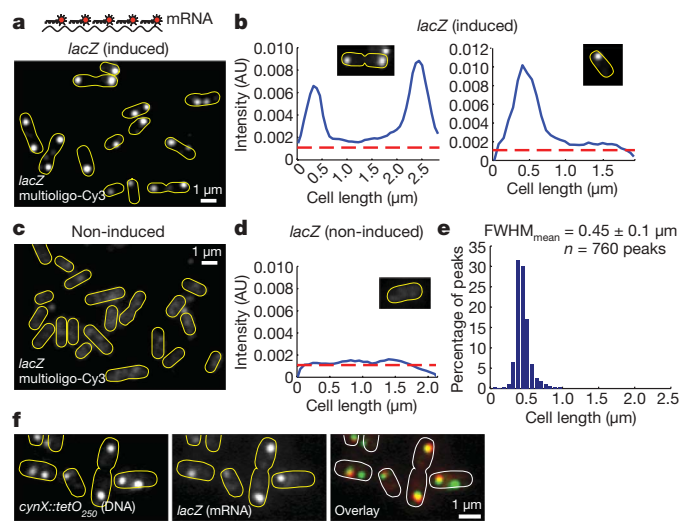

Figure 3 | Endogenous LacZ-encoding mRNAs display diffraction-limited dispersion from sites of transcription in *E. coli*. a, RNA-FISH of wild-type MG1655 *E. coli* cells using 48 Cy3-labelled DNA probes complementary to the *lacZ* mRNA sequence after 20 min of IPTG induction. **b,** Representative FISH intensity profiles of *lacZ* mRNA signal in individual MG1655 cells. The red dashed line represents the background fluorescence from non-induced cells. **c,** Visualization of background fluorescence in non-induced MG1655 cells using conditions as in (**a**). **d,** Representative fluorescence intensity profiles of individual non-induced cells. The red dashed line represents background fluorescence from non-induced cells. **e,** Histogram of FWHM values of *lacZ* mRNA signals from IPTG-induced cells. **f,** Co-visualization of a chromosomal *tetO₂₅₀* array (inserted into the *cynX* locus adjacent to the *lac* operon) and the *lacZ* mRNA signal in DL2875 *E. coli* cells.
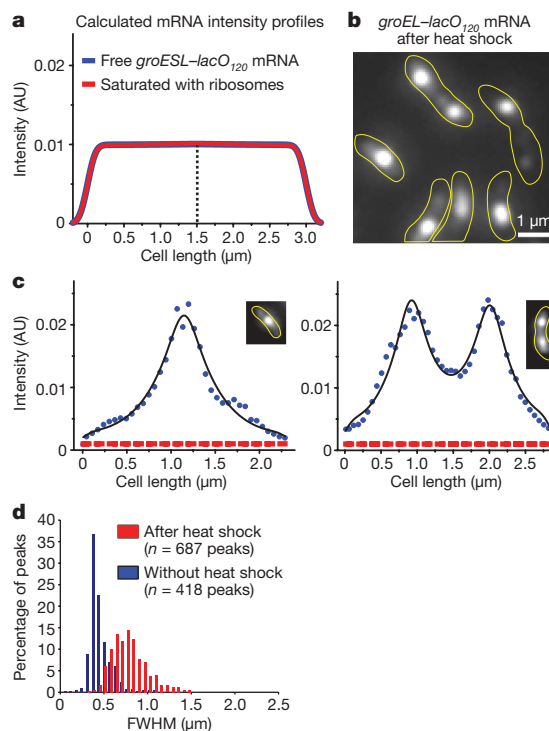

Figure 4 | Dispersion of *groESL–lacO₁₂₀* mRNA. a, Spatial distribution profiles of the 6.3-kb *groESL–lacO₁₂₀* mRNA distribution profiles in a 3-μm virtual cell calculated with equation (6) (Supplementary Information), assuming that *groESL–lacO₁₂₀* mRNA is freely diffusible and either ribosome-free (blue) or saturated with ribosomes (red). The dotted line delineates the source of mRNA (site of transcription). **b,** RNA-FISH image of lacO–Cy3-hybridized *groESL–lacO₁₂₀* mRNAs in CJW2966 cells after 15 min at 42 °C. **c,** Representative lacO–Cy3 hybridized-*groESL–lacO₁₂₀* mRNA intensity profiles of individual, heat-shocked CJW2966 cells. The blue dots are the experimental data and the black line is the best fit using the two-source (*right*) or one-source (*left*) model (see Supplementary Information). The red dashed line corresponds to the background fluorescence. **d,** Histogram of FWHM values of *groESL–lacO₁₂₀* mRNA from fluorescence intensity profiles of CJW2966 cells grown at 30 °C (blue) or after heat shock (42 °C for 15 min; red).

(Fig. 4d)). We obtained almost perfectly overlapping distributions of mRNA dispersion and levels (Supplementary Fig. 7a, b) when examining the natural *groESL* mRNA in wild-type cells using a single internal groEL probe, which validates our observations. Under these heat-shock conditions, northern blot analysis shows that *groESL* mRNA accumulates as a full-length species[13]. Furthermore, the rate of mRNA decay was largely unaffected by heat shock (Supplementary Fig. 2d; see also Supplementary Information for real-time PCR measurements). It is possible that the large number of *groESL* transcripts saturates the supposed interactions that limit dispersion. In any case, these results indicate that although mRNAs are indeed able to diffuse, their dispersion remains limited, yielding an apparent diffusion coefficient $D_a = 0.0005 \pm 0.0003\,\mu m^2\,s^{-1}$ (see Supplementary Information). This value is two to three orders of magnitude lower than estimates in the literature[6,7] and from our modelling for freely diffusing transcripts (Supplementary Information).

Importantly, our results indicate that there is little mixing of mRNA species inside the cell. Because the chromosome is spatially organized, with each gene occupying a specific cellular address[23], limited mRNA dispersion implies that translation and thus protein synthesis are spatially organized, according to chromosomal gene order.

mRNA and ribosomal mobility in *C. crescentus*

In *C. crescentus*, DNA and ribosomes spread throughout the cell[24], which we confirmed by co-visualizing 4′,6-diamidino-2-phenylindole (DAPI) staining and the functional ribosomal protein fusion L1–GFP
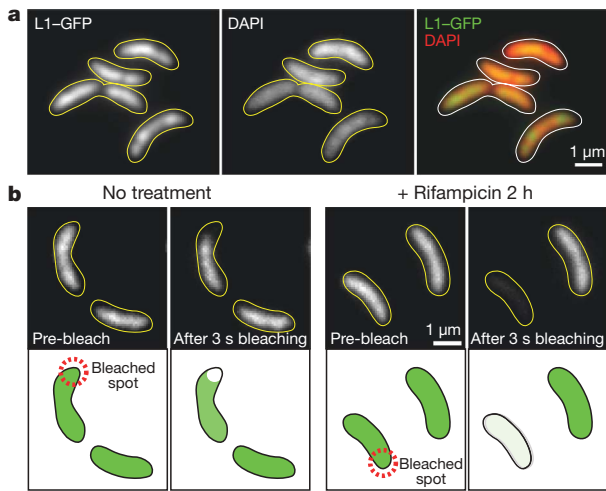
Figure 5 | mRNA limits diffusion of translating ribosomes. a, Co-visualization of L1–GFP and DNA (DAPI) in CJW3365 cells. **b,** Fluorescence loss in photobleaching experiment. A 3.3-s laser pulse was used to bleach a small region of CJW3365 cells producing L1–GFP, either without (left) or with (right) rifampicin pre-treatment.

produced under native conditions (Fig. 5a). Our findings predict that translating ribosomes should display little mobility by virtue of their interaction with mRNAs, whereas free ribosomal subunits should diffuse rapidly. Consistent with this notion, photobleaching a small region of cells with a laser pulse series of 3 s caused a distinct clearance of the L1–GFP signal within the illuminated region (Fig. 5b), whereas unbleached regions of the same cells retained about 82% ± 7% (n = 28) of their original fluorescence signal. When mRNAs were depleted by 2 h of rifampicin treatment, there was no distinct clearance of signal, but instead a general, uniform loss in fluorescence occurred throughout the cells (Fig. 5b) owing to rapid motion of ribosomal material into the illuminated spot during the 3 s laser pulse. Shorter rifampicin treatments also caused severe loss in fluorescence in unbleached regions (Supplementary Fig. 8a). The levels of ribosomal RNA were similar in all conditions tested (Supplementary Fig. 8b). The observation that about 18% of fluorescent signal is lost from the unbleached regions when the mRNA is present (that is, in untreated cells) agrees remarkably well with biochemical estimates of ~80% of the ribosomal material being actively engaged in translation[25]. Collectively, our data show that actively translating ribosomes are unable to diffuse freely because of mRNA localization.

In some bacteria like *Bacillus subtilis*, ribosomes are enriched around the nucleoid (that is, cell periphery including poles)[26]; rifampicin treatment abolishes this accumulation[27]. Thus, bacteria can differ in their nucleoid organization, with some bacteria (for example, *B. subtilis*) preferentially exposing their actively transcribing regions to the cell periphery whereas others (for example, *C. crescentus*) transcribe throughout the nucleoid region. Nonetheless, the observation that rifampicin causes dispersion of ribosomal material in *B. subtilis*[27] is consistent with mRNAs also displaying limited dispersion in this organism.

RNase E spatial organization in *C. crescentus*

Besides transcription and translation, mRNA decay is the other very important mRNA process in the flow of genetic information. RNase E is a major component of the RNA degradosome in *E. coli*[28] and in *C. crescentus*, a functional RNase E–mGFP (RNase E fused to monomeric green fluorescence protein) fusion (synthesized from the native *rne* promoter on the chromosome in place of RNase E) exhibited a somewhat patchy localization pattern throughout the cell (Fig. 6a). This pattern is not incompatible with the proposed helical distribution of RNase E in *E. coli*[29] as the narrow cell width of *C. crescentus* cells (~0.5 μm) hampers resolution of three-dimensional patterns. *E. coli* RNase E also displays an affinity for the membrane[30]. Importantly, we found that the cellular localization of RNase E in *C. crescentus* was determined by the location of the DNA. This was demonstrated by using a double temperature sensitive *parE ftsA* mutant that filaments and produces large cytoplasmic DNA-free regions at the restrictive temperature[31]. Under these conditions, RNase E–mGFP colocalized with the DNA and was absent from the cytoplasmic DNA-free regions of the filamentous mutant (Fig. 6b). Notably, this striking colocalization was not simply the result of mRNA substrate availability for RNase E in the DNA regions since it was preserved in mRNA-depleted cells that had been treated with rifampicin for 2 h (Fig. 6c). Instead, this result suggests that RNase E directly or indirectly associates with the DNA (possibly through components of the RNA degradosome and/or DNA-binding proteins). It should be noted that RNase E–mGFP localization appeared substantially more punctuated within the DNA region in mRNA-depleted cells (Fig. 6c), indicating that 'hot' spots of association may exist and that mRNA substrate availability has some influence on RNase E cellular distribution. In wild-type cells, the DNA is estimated to occupy only a few percent of the cytoplasmic space[32]. An association between DNA and RNase E would thus suggest that mRNA decay is also spatially organized according to chromosomal organization.
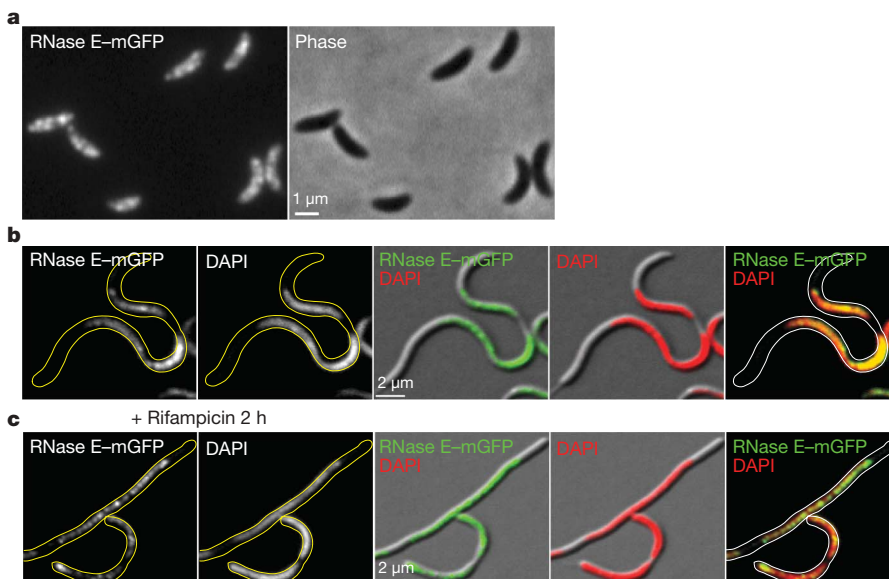

Figure 6 | RNase E colocalizes with the DNA in *C. crescentus*. a, Fluorescence and corresponding phase micrographs of CJW3100 cells producing RNase E–mGFP. **b,** Co-visualization of RNase E–mGFP and DNA (DAPI) in CJW3099 cells grown at the restrictive temperature (37 °C) for 4 h to produce large DNA-free regions. **c,** Same as (**b**) except after rifampicin pre-treatment.

Discussion

The spatial organization of mRNA implies that the cell interior is functionally compartmentalized so that specific protein species are produced within small subcellular regions defined by the genetic map and organization of the chromosome. This spatial organization may have implications for the cell. For instance, genes encoding interacting proteins frequently cluster and thus conservation of gene proximity has been a useful tool for predicting functional interactions. Yet the selective pressure for the conservation of gene clustering has remained elusive, as horizontal transfer and co-regulation through operon organization cannot solely account for the observed level of gene clustering in bacterial genomes[33,34]. Using the chromosome as a spatial organizer of mRNA may provide a basis for gene clustering. Our findings suggest that interacting proteins encoded by clustered genes are synthesized in the same vicinity, which may facilitate rapid interaction, possibly even as they are produced. This might be particularly important when complex formation increases the stability of the individual components.

Our findings indicate that, despite lacking internal organelles, bacteria can spatially organize mRNA processes essential for the transfer of genetic information, in a drastically different way from eukaryotes. Rather than using separate functional compartments (such as the nucleus, cytoplasm and P-bodies), *C. crescentus* uses chromosome organization as a master template to organize not only transcription, but also translation and probably mRNA decay in the cellular space. This centralized, chromosome-centric organizational strategy introduces a greater order to the way mRNA processes need to be conceptualized and studied, as current models of gene expression do not make any spatial considerations and assume that translation and decay of any particular mRNA are uniform in space.

METHODS SUMMARY

RNA and DNA FISH microscopy was performed on bacterial cells to determine the location of mRNAs and gene loci, respectively. Custom MATLAB software and mathematical modelling were used to estimate the dispersion of mRNA inside the cytoplasm. We used fluorescent microscopy to determine the localization of fluorescently labelled RNase E and ribosomal protein L1 in living cells. We performed fluorescence recovery after photobleaching (FRAP) microscopy to determine the mobility of L1–GFP in living cells. A detailed description of the image analysis can be found in the Supporting Information.

Full Methods and any associated references are available in the online version of the paper at www.nature.com/nature.

1. Passalacqua, K. D. *et al.* Structure and complexity of a bacterial transcriptome. *J. Bacteriol.* **191**, 3203–3211 (2009).
2. Epshtein, V. & Nudler, E. Cooperation between RNA polymerase molecules in transcription elongation. *Science* **300**, 801–805 (2003).
3. Vogel, U. & Jensen, K. F. The RNA chain elongation rate in *Escherichia coli* depends on the growth rate. *J. Bacteriol.* **176**, 2807–2813 (1994).
4. Bernstein, J. A., Khodursky, A. B., Lin, P. H., Lin-Chao, S. & Cohen, S. N. Global analysis of mRNA decay and abundance in *Escherichia coli* at single-gene resolution using two-color fluorescent DNA microarrays. *Proc. Natl Acad. Sci. USA* **99**, 9697–9702 (2002).
5. Miller, O. L. Jr, Hamkalo, B. A. & Thomas, C. A. Jr. Visualization of bacterial genes in action. *Science* **169**, 392–395 (1970).
6. Guet, C. C. *et al.* Minimally invasive determination of mRNA concentration in single living bacteria. *Nucleic Acids Res.* **36**, e73 (2008).
7. Golding, I. & Cox, E. C. RNA dynamics in live *Escherichia coli* cells. *Proc. Natl Acad. Sci. USA* **101**, 11310–11315 (2004).
8. Maamar, H., Raj, A. & Dubnau, D. Noise in gene expression determines cell fate in *Bacillus subtilis*. *Science* **317**, 526–529 (2007).
9. Golding, I., Paulsson, J., Zawilski, S. M. & Cox, E. C. Real-time kinetics of gene activity in individual bacteria. *Cell* **123**, 1025–1036 (2005).
10. Valencia-Burton, M., McCullough, R. M., Cantor, C. R. & Broude, N. E. RNA visualization in live bacterial cells using fluorescent protein complementation. *Nature Methods* **4**, 421–427 (2007).
11. Pilhofer, M., Pavlekovic, M., Lee, N. M., Ludwig, W. & Schleifer, K. H. Fluorescence *in situ* hybridization for intracellular localization of *nifH* mRNA. *Syst. Appl. Microbiol.* **32**, 186–192 (2009).
12. Valencia-Burton, M. *et al.* Spatiotemporal patterns and transcription kinetics of induced RNA in single bacterial cells. *Proc. Natl Acad. Sci. USA* **106**, 16399–16404 (2009).
13. Avedissian, M. & Lopes Gomes, S. Expression of the *groESL* operon is cell-cycle controlled in *Caulobacter crescentus*. *Mol. Microbiol.* **19**, 79–89 (1996).
14. Lim, F. & Peabody, D. S. Mutations that increase the affinity of a translational repressor for RNA. *Nucleic Acids Res.* **22**, 3748–3752 (1994).
15. Lau, I. F. *et al.* Spatial and temporal organization of replicating *Escherichia coli* chromosomes. *Mol. Microbiol.* **49**, 731–743 (2003).
16. Deana, A. & Belasco, J. G. Lost in translation: the influence of ribosomes on bacterial mRNA decay. *Genes Dev.* **19**, 2526–2533 (2005).
17. Viollier, P. H. & Shapiro, L. Spatial complexity of mechanisms controlling a bacterial cell cycle. *Curr. Opin. Microbiol.* **7**, 572–578 (2004).
18. Wheeler, R. T. & Shapiro, L. Differential localization of two histidine kinases controlling bacterial cell differentiation. *Mol. Cell* **4**, 683–694 (1999).
19. Mangan, E. K. *et al.* FlbT couples flagellum assembly to gene expression in *Caulobacter crescentus*. *J. Bacteriol.* **181**, 6160–6170 (1999).
20. Yarchuk, O., Jacques, N., Guillerez, J. & Dreyfus, M. Interdependence of translation, transcription and mRNA degradation in the *lacZ* gene. *J. Mol. Biol.* **226**, 581–596 (1992).
21. Derman, A. I., Lim-Fong, G. & Pogliano, J. Intracellular mobility of plasmid DNA is limited by the ParA family of partitioning systems. *Mol. Microbiol.* **67**, 935–946 (2008).
22. Elowitz, M. B., Surette, M. G., Wolf, P. E., Stock, J. B. & Leibler, S. Protein mobility in the cytoplasm of *Escherichia coli*. *J. Bacteriol.* **181**, 197–203 (1999).
23. Viollier, P. H. *et al.* Rapid and sequential movement of individual chromosomal loci to specific subcellular locations during bacterial DNA replication. *Proc. Natl Acad. Sci. USA* **101**, 9257–9262 (2004).
24. Briegel, A. *et al.* Multiple large filament bundles observed in *Caulobacter crescentus* by electron cryotomography. *Mol. Microbiol.* **62**, 5–14 (2006).
25. Forchhammer, J. & Lindahl, L. Growth rate of polypeptide chains as a function of the cell growth rate in a mutant of *Escherichia coli* 15. *J. Mol. Biol.* **55**, 563–568 (1971).
26. Lewis, P. J., Thaker, S. D. & Errington, J. Compartmentalization of transcription and translation in *Bacillus subtilis*. *EMBO J.* **19**, 710–718 (2000).
27. Mascarenhas, J., Weber, M. H. & Graumann, P. L. Specific polar localization of ribosomes in *Bacillus subtilis* depends on active transcription. *EMBO Rep.* **2**, 685–689 (2001).
28. Carpousis, A. J., Luisi, B. F. & McDowall, K. J. Endonucleolytic initiation of mRNA decay in *Escherichia coli*. *Prog Mol Biol Transl Sci* **85**, 91–135 (2009).
29. Taghbalout, A. & Rothfield, L. RNaseE and the other constituents of the RNA degradosome are components of the bacterial cytoskeleton. *Proc. Natl Acad. Sci. USA* **104**, 1667–1672 (2007).
30. Khemici, V., Poljak, L., Luisi, B. F. & Carpousis, A. J. The RNase E of *Escherichia coli* is a membrane-binding protein. *Mol. Microbiol.* **70**, 799–813 (2008).
31. Ward, D. & Newton, A. Requirement of topoisomerase IV *parC* and *parE* genes for cell cycle progression and developmental regulation in Caulobacter crescentus. *Mol. Microbiol.* **26**, 897–910 (1997).
32. Neidhart, F. C. & Umbarger, H. E. in *Escherichia coli and Salmonella: cellular and molecular biology* 2nd edition, Vol. 1 (ed. Neidhardt, F. C.) Ch. 3, 13–16 (ASM Press, 1996).
33. Tamames, J. Evolution of gene order conservation in prokaryotes. *Genome Biol.* **2**, research0020.1–research0020.11 (2001).
34. Fang, G., Rocha, E. P. & Danchin, A. Persistence drives gene clustering in bacterial genomes. *BMC Genomics* **9**, 4 (2008).

Author Contributions C.J.-W., P.M.L. and A.F.J. designed experiments. P.M.L. performed the FISH, ribosome and RNaseE experiments, and analysed FISH and FRAP data. A.F.J. carried out the MS2 experiments and analysed the data. P.M.L. and J.H. performed the real-time PCR measurements. O.S. developed the tools for image and data analysis. I.S. described and implemented the mathematical model for the analysis of mRNA diffusion. T.E. provided conceptual and data analysis advice. C.J.-W., P.M.L. and A.F.J. wrote the paper.

Author Information Reprints and permissions information is available at www.nature.com/reprints. The authors declare no competing financial interests. Readers are welcome to comment on the online version of this article at www.nature.com/nature. Correspondence and requests for materials should be addressed to C.J.-W. (christine.jacobs-wagner@yale.edu).

METHODS

Bacterial strains, plasmids and growth. *C. crescentus* cultures were grown at 30 °C (other temperatures when indicated) in PYE (peptone yeast extract) or M2G$^+$ (phosphate-buffered minimal medium supplemented with glucose plus 1% PYE) medium supplemented with antibiotics or sugars (0.03% xylose or 0.2% glucose) as indicated[35]. *C. crescentus* cultures used in this study were in exponential phase of growth. Synchronizations of cell populations with respect to the cell cycle were performed as described[36]. *E. coli* strains were grown at 37 °C in Luria–Bertani or M9 glycerol media supplemented with the appropriate antibiotics. Transformations, conjugations and transductions were performed as described previously[35]. Expression from *Pxyl* or *Pvan* was achieved by adding 0.03% xylose or 0.5 mM vanillic acid, respectively, except in indicated cases where 0.3% xylose was used. Depletion of mRNA was achieved by treatment with rifampicin (200 µg ml^{-1}) for the indicated amount of time, and rifampicin was also present on the agarose-padded slides for the RNase E and L1–GFP experiments.

Strains and plasmids are listed in Supplementary Table 1; see below for their mode of construction.

Fluorescence *in situ* hybridization (FISH). DNA FISH was performed as described previously[37]. For RNA-FISH, we used the following protocol: cells growing in PYE were fixed in 4% formaldehyde solution (4% formaldehyde and 30 mM NaHPO$_3$ pH 7.5) for 15 min at room temperature and 30 min on ice. The samples were spun down three times at 6,000 r.p.m. (3,000*g*) for 3 min and washed in 1× DEPC-treated PBS. The cell pellets were resuspended in 100 µl GTE buffer (50 mM glucose, 20 mM Tris-HCl pH 7.5, 10 mM EDTA pH 8). Four microlitres of 10 µg ml^{-1} lysozyme solution (GTE, 4 mM vanadyl ribonucleoside complex (VRC), 10 µg ml^{-1} lysozyme) were added to 12 µl of cell suspension. The mixture was immediately placed onto poly-L-lysine-coated multi-well slides, and incubated for 10 min at room temperature. The excess liquid was aspirated and the slides were left 1 min to dry before putting them in −20 °C methanol for 10 min. Next, the slides were dipped in −20 °C acetone for 30 s. Once the slides were dry, they were incubated at 37 °C for 30–60 min in a 40% formamide solution (40% formamide, 2× DEPC-treated saline-sodium citrate buffer (SSC)). LNA probe was added to the hybridization solution I (80% formamide, 1 mg ml^{-1} *E. coli* tRNA, 2× DEPC-treated SSC, 70 µg ml^{-1} calf-thymus DNA) at a final concentration of 250 nM, and incubated at 80 °C for 5 min before mixing with the hybridization solution II (20% dextran sulphate, 4 mM VRC, 40 U RNase inhibitor, 0.2% RNase-free BSA, 2× DEPC-treated SSC) in a 1:1 ratio. The hybridization solution (25 50 µl) was added to each well of the slide and hybridized for 2–3 h. The slides were then washed twice in 50% formamide and 2× DEPC-treated SSC solution for 30 min and briefly rinsed five times in DEPC-treated PBS. Four microlitres of DAPI (1.5 µg ml^{-1}) in SlowFade solution (Invitrogen) were added to each well and the slide was covered and sealed using clear nail polish. The slides were either visualized immediately or stored in the dark at −20 °C. Probe sequences are provided below.

For the dual DNA/mRNA localization experiments in *C. crescentus*, we used different methods. In the case of *C. crescentus groESL–lacO$_{120}$*, the DNA sequence was detected by immunofluorescence microscopy using anti-GFP antibodies after 15-min induction of LacI–CFP (LacI fused to cyan fluorescent protein) synthesis with 0.03% xylose in the presence of 50 µM IPTG, whereas the corresponding *groESL–lacO$_{120}$* mRNA was detected by RNA FISH using the lacO–Cy3 probe. Co-visualization of *creS-lacO$_{120}$* mRNA and *tetO$_{240}$*-tagged origin of replication, which is close (∼40 kb) to the *creS* region, was achieved by using DNA-FISH with the tetO–Alexa488 probe followed by RNA-FISH with the lacO–Cy3 probe. For the *E. coli* experiments, the *cynX* locus adjacent to the *lac* operon was detected by using DNA-FISH with the tetO–Alexa488 probe followed by RNA-FISH with the Cy3-labelled *lacZ* multi-oligonucleotides to covisualize *lacZ* mRNA.

Light and immunofluorescence microscopy. Microscopy was performed using a Nikon E1000 microscope equipped with ×100 differential interference contrast (DIC) and phase contrast objectives and a Hamamatsu Orca-ER camera, or a Nikon E80i microscope with ×100 phase contrast objective and a Hamamatsu Orca II-ER camera. For immobilization and live cell visualization, cells were placed on a 1% agarose pad containing growth medium and antibiotics and inducers when appropriate. For FISH experiments, fixed cells were placed and permeabilized on poly-L-lysine-coated slides.

Immunofluorescence microscopy was performed as described[38] using JL8 anti-GFP monoclonal antibody (Clonotech; 1:1,000 dilution) and goat anti-mouse-FITC secondary antibody (Jackson Laboratories; 1:10,000 dilution). After this, the cells were re-fixed in 4% formaldehyde solution for 5 min at room temperature, and FISH was performed as described above. The green and red microspheres were obtained from Molecular Probes.

For the photobleaching experiments, we used a Photonics Targeting Illumination system controlled by MetaMorph. Fluorescence photobleaching was performed by illumination at 488 nm. Image acquisition was obtained using a Nikon 80i with a ×100 phase contrast objective and an EM-CCD Andor camera.

Immunoblotting. Cultures grown under appropriate conditions were normalized by absorbance at 660 nm. Approximately 250 µl samples of each culture were pelleted, resuspended in loading buffer, and electrophoretically resolved by 12% SDS–polyacrylamide gel electrophoresis. The gels were electro-transferred to polyvinylidene difluoride membranes, which were probed with anti-GFP (Clontech; 1:1,000 dilution).

35. Ely, B. Genetics of *Caulobacter crescentus*. *Methods Enzymol.* **204**, 372–384 (1991).
36. Evinger, M. & Agabian, N. Envelope-associated nucleoid from *Caulobacter crescentus* stalked and swarmer cells. *J. Bacteriol.* **132**, 294–301 (1977).
37. Jensen, R. B. & Shapiro, L. The *Caulobacter crescentus smc* gene is required for cell cycle progression and chromosome segregation. *Proc. Natl Acad. Sci. USA* **96**, 10661–10666 (1999).
38. Domian, I. J., Quon, K. C. & Shapiro, L. Cell type-specific phosphorylation and proteolysis of a transcriptional regulator controls the G1-to-S transition in a bacterial cell cycle. *Cell* **90**, 415–424 (1997).